Towards Visual-Inertial Navigation of an Underwater Vehicle for Aquaculture Inspection Operation

Svetlana Potyagaylo[1] and Savvas G. Loizou[1]

***Abstract*— This paper presents an online sensor fusion algorithm for state estimation of a remotely operated underwater vehicle for aquaculture inspection. The algorithm is based on an Unscented Kalman Filer (UKF) and uses information from several sources including an onboard inertial sensor, an onboard camera combined with line lasers and a priory knowledge about the aquaculture geometry. The performance of the fusion algorithm is validated through several Monte Carlo simulation scenarios for a small-scale aquaculture installation under realistic environmental parameters.**

I. Introduction

Aquaculture and fisheries are agricultural sub-domains where application of robotic technologies is expected to significantly contribute to their future development and sustainability. The current work is part of an ongoing research project co-funded by the European Regional Development Fund and the Republic of Cyprus and aimed at developing an autonomous system for visual inspection of fish farm nets and moorings by using a tethered Remotely Operated Vehicle (ROV) in a shared autonomy mode.

Underwater robotic operations in the proximity of underwater structures like aquaculture fish-nets face the challenging problem of localization, since this is a GPS-denied environment. In this work, we address a problem of localization and state estimation of the ROV with respect to the aquaculture by fusing information from different sources. In this paper, three information sources were assumed to be used for the position estimation of the ROV: the Inertial Measurement Unit (IMU), the novel combined Laser Vision System (LVS), and the depth pressure sensor along with a priory knowledge of the aquaculture geometry. Such a set of sensors can be considered as a minimum set of sensors that represents a baseline performance benchmark. By incorporating measurements from other available sensors (such as a magnetic sensor or optical flow technique) that will come on top of the mentioned sensors, we can expect improvements on estimation accuracy.

II. System Overview

The ROV used in the project is a VideoRay Pro IV ROV equipped with two horizontal thrusters for surge and yaw motions and one vertical thruster for heave motion. The vehicle is under-actuated, meaning that it cannot perform sway, roll and pitch motions. The basic sensor system includes a front facing camera housed with an acrilic dome, an IMU, magnetometer and depth sensors. In addition to these sensors, the ROV was equipped with three line lasers. The combined LVS is shown on Fig. 1.

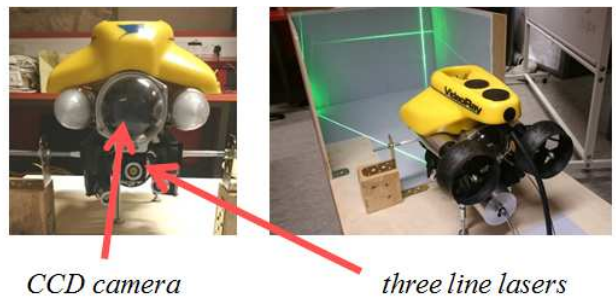

Fig. 1. The Combined Laser Vision system setup.

We consider the ROV as a 6-DOF rigid body that can be described by the following system of equations [1]:

$$\begin{aligned} \mathbf{M}\dot{\boldsymbol{\nu}} + \mathbf{C}\left(\boldsymbol{\nu}\right)\boldsymbol{\nu} + \mathbf{D}\left(\boldsymbol{\nu}\right)\boldsymbol{\nu} + \mathbf{g}\left(\boldsymbol{\eta}\right) = \boldsymbol{\tau}, \\ \dot{\boldsymbol{\eta}} = \mathbf{J}\left(\boldsymbol{\eta}\right)\boldsymbol{\nu}, \end{aligned} \tag{1}$$

where $\mathbf{M}$ is the inertia matrix, $\boldsymbol{\nu} = [u, v, w, p, q, r]^T$ is the body linear and angular velocities, $\mathbf{C}$ is the coriolis and centripetal matrix, $\mathbf{D}$ is the drag matrix, $\mathbf{g}$ is the force vector, $\boldsymbol{\tau}$ is the trust vector, $\boldsymbol{\eta} = [x, y, z, \phi, \theta, \psi]^T$ is the position and Euler angles vector, $\mathbf{J}$ is the transformation matrix.

The IMU sensor used in this work consists of three-axis accelerometer and gyro providing measurements of the linear accelerations $\mathbf{a}$ in the body frame and the angular velocity $\boldsymbol{\nu}_2$ in the body frame of the ROV. The IMU is modeled as a function h_{LVS} of the ROV's state along with the additive noise with zero mean and covariance matrix $\mathbf{R}_{IMU}$. The depth pressure sensor is modeled as h_{PS} based on the Pascal's Law for the hydrostatic pressure that is the force exerted on an object due to the weight of water above it and provides the measurements of the current ROV's depth z corrupted by the additive zero mean noise with covariance $\mathbf{R}_{PS}$.

The LVS sensor consists of a CCD camera and a set of three lasers projecting the lines in the form of a triangle on the target as shown on Fig. 1. The CCD camera is enclosed by a hemispherical dome. Since the acrylic dome and an underwater environment affect the vision system of the ROV, a special camera calibration process was used [2].

*This work was co-funded by the European Regional Development Fund and the Republic of Cyprus through the Research Promotion Foundation under research grant ΑΕΙΦΟΡΙΑ/ΓΕΩΡΓΟ/0311(BIE)/08

[1]S. Potyagaylo and S. Loizou are with Mechanical and Materials Science and Engineering Department, Cyprus University of Technology, Limassol 3041, CYPRUS svetlana.potyagaylo, savvas.loizou@cut.ac.cy

The model of the aquaculture [3] consisting of fish net cages and mooring lines was created as well. The model was used offline to calculate the aquaculture geometry for different environmental conditions. During the operation, the fish net geometry model $\mathcal{F}$ represented as a quad mesh is served as a priory available information for the LVS model h_{LVS} that provides the distance and orientation of the aquaculture in form of the normal vector of the closest mesh of $\mathcal{F}$. The additive noise with zero mean and covariance $\mathbf{R}_{LVS}$ is assumed as well.

III. Asynchronous Unscented Kalman Filter Algorithm

In this work, we applied an UKF scheme to estimate the states of the vehicle. Since the measurements from the IMU, pressure and LVS sensors could arrive with different frequencies and asynchronously, the UKF algorithm was modified to incorporate this feature using the approach similar to [4]. The system process model is predicted forward in time and the mean and covariance of the state vector are updated only when a new measurement from either of the sensors is available. In the case, when only the IMU/Pressure sensor/LVS measurements were received, the measurement model for the UKF algorithm is formulated as h_{IMU}, h_{PS}, or h_{LVS}, respectively. However, when the measurements from two or more sensors are available, the combination of the sensors models is used. For example, for all three sensors of the vehicles, the threefold measurement model can be written as:

$$\mathbf{x} = \begin{bmatrix} h_{IMU}(\mathbf{x}) + \mathbf{w}_{IMU} \\ h_{PS}(\mathbf{x}) + \mathbf{w}_{PS} \\ h_{LVS}(\mathbf{x}) + \mathbf{w}_{LVS} \end{bmatrix} \qquad (2)$$

In this case, the sensor noise covariance matrix used in the UKF update step should be rewritten as well in accordance to the applied sensor model.

IV. Simulation Results

The developed UKF approach was validated through various simulations under realistic levels of noises and disturbances. The hydrodynamic and inertia parameters of the ROV were assumed to be equal to the parameters of the VideoRay ROV III [5]. The IMU sensor provides measurements at a frequency of $100\,\mathrm{Hz}$. The pressure sensor frequency is $100\,\mathrm{Hz}$, while the LVS sensor was assumed to provide data with the frequency of $10\,\mathrm{Hz}$.

The simulation scenario was to navigate the vehicle downwards along the aquaculture with the constant vertical velocity $w = 0.1\,\mathrm{m/s}$. Simple controllers were applied in order to keep the vehicle along the predefined trajectory and the aquaculture in the field of view of the ROV. The STD of the gyro, accelerometers, pressure sensor and LVS measurements were assumed as $0.05\,\mathrm{rad/s}$, $0.03\,\mathrm{m/s}$, $0.1\,\mathrm{m}$, $0.1\,\mathrm{m}$, repectively. A series of Monte-Carlo runs were conducted in order to evaluate the performance of the proposed sensor fusion algorithm for the position estimation only. Two metrics were used to examine the filter, namely, the root mean squared error (RMSE), to estimate the accuracy of the filter, and the normalized estimation error squared (NEES), to provide a measure of the filter consistency [6]. The average NEES (ANEES) over 10 Monte-Carlo runs and for each time step i is shown on Fig. 2(a) for $100\,\mathrm{s}$ simulation run. The average of the NEES over all Monte-Carlo runs and all times steps was 11.16. According to [7], the performance of the asynchronous UKF applied in this work is close to the performance of the standard UKF. The RMSE is shown on Fig. 2(b) while the average RMSE over all steps for this case was $0.65\,\mathrm{m}$.

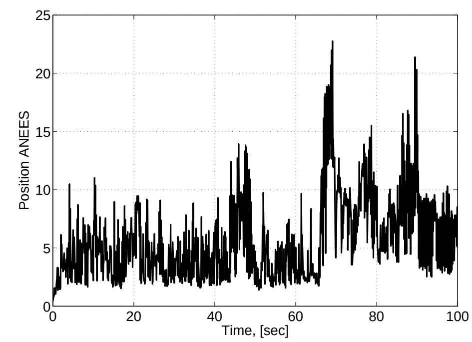

(a) The position ANEES averaged per time step

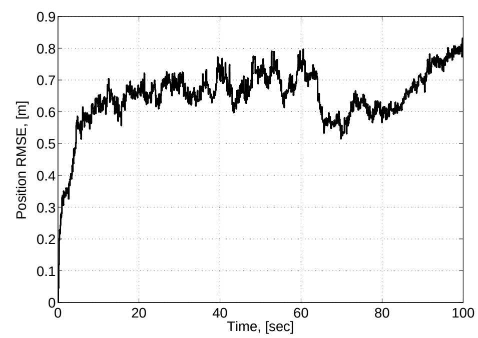

(b) The position RMSE averaged per time step.

Fig. 2. Simulation results for 10 Monte-Carlo runs.

References

[1] T. I. Fossen, *Guidance and Control of Ocean Vehicles*. New York: Wiley, 1994.

[2] C. C. Constantinou, S. G. Loizou, G. Georgiades, S. Potyagaylo, and D. Skarlatos, "Adaptive Calibration of an Underwater Robot Vision System based on Hemispherical Optics," in *Autonomous Underwater Vehicles Conference (AUV)*, October 2014.

[3] S. Potyagaylo and S. G. Loizou, "Online Adaptive Geometry Predictor of Aquaculture Fish-Nets," in *Mediterranean Conference on Control and Automation (MED)*, June 2014.

[4] G. C. Karras, S. G. Loizou, and K. J. Kyriakopoulos, "Towards Semi-autonomous Operation of Under-actuated Underwater Vehicles: Sensor Fusion, On-line Identification and Visual Servo Control," *Autonomous Robots*, vol. 31, no. 1, pp. 67–86, 2011.

[5] W. Wang and C. M. Clark, "Modeling and Simulation of the VideoRay Pro III Underwater Vehicle," in *OCEANS*, 2006.

[6] Y. Bar-Shalom, X. R. Li, and T. Kirubarajan, *Estimation with Applications to Tracking and Navigation*. New York: Wiley, 2001.

[7] G. P. Huang, A. I. Mourikis, and S. I. Roumeliotis, "A Quadratic-Compexity Observability-Constrained Uscented Kalman Filter for SLAM," *IEEE Transactions on Robotics*, vol. 29, no. 5, pp. 1226–1243, 2013.